ISSN 2070-0482, Mathematical Models and Computer Simulations, 2014, Vol. 6, No. 4, pp. 342–350. © Pleiades Publishing, Ltd., 2014.
Original Russian Text © I.B. Petrov, N.I. Khokhlov, 2014, published in Matematicheskoe Modelirovanie, 2014, Vol. 26, No. 1, pp. 83–95.

Modeling of 3d Seismic Problems Using High-Performance Computing Systems

I. B. Petrov and N. I. Khokhlov

Moscow Institute of Physics and Technology (State University), Moscow, Russia

e-mail: k_h@inbox.ru

Received September 10, 2012

Abstract—This paper examines some issues in numerical modeling of seismology in three-dimensional space on high-performance computing systems. As a method of modeling, the grid-characteristic method is used. This method allows accurate staging of different contact conditions and is suitable for the most physically correct solutions of problems of seismology and seismic prospecting in complex heterogeneous media. We use the grid-characteristic schemes up to the 4th order accuracy inclusive. The software package is parallelized for work in a distributed clustered medium using the MPI technology. We present the results of the simulation of the Love and Rayleigh surface seismic waves, as well as the passage of seismic waves initiated by an earthquake's hypocenter to the earth's surface through a multilayer geological formation.

Keywords: computer simulation, systems of hyperbolic equations, highly productive computations, MPI, surface seismic waves

DOI: 10.1134/S2070048214040061

1. INTRODUCTION

Here we consider some issues in the numerical simulation of some problems in the propagation of wave disturbances in layered geological media on high performance computing systems. The physical sizes of the areas of integration in problems of this kind may achieve dozens and hundreds of kilometers. For the correct modeling of wave disturbances at such distances, high precision numerical methods are needed that account for the wave properties of the equations at hand and have the possibility of simulating complicated dynamic processes in nonhomogenous geological media with a set of contact and free boundaries. As such a method, the grid-characteristic method [1] is used here for the numerical solution of the systems of equations of the mechanics of a deformed solid body. This method allows application of monotonic difference schemes of a higher order of accuracy [2], construction of the correct numerical algorithms on the boundaries of domains of integration and on contact boundaries [3]. For some problems of seismics, this method has already been used in the two-dimensional case [4]; in this work modeling was performed in the three-dimensional statement.

For correct assignment of large domains of modeling, three-dimensional computational grids with a sufficient number of nodes are used. The computations on such grids require more CPU time and computer memory resources; to accelerate the computation process, the MPI [5] technology has been used in this work, which allows the program to work on larger grids (up to 1 billion nodes).

As an example of the problems solved, the results of modeling the Rayleigh and Love surface seismic waves and their comparison with the theory are presented. The propagation of elastic seismic waves through a multilayer geological formation is considered; the propagation of disturbances from the hypocenter of the earthquake to the surface is modeled.

2. MATHEMATICAL MODEL

2.1. Determining equations. We formulate equations of the linear dynamic theory of elasticity, which is obeyed by the state of infinitely small volume of the linear-elastic medium. We consider the nonstationary

equations of the theory of elasticity for the case of three variables in the orthonormal system of coordinates (x_1, x_2, x_3):

$$\begin{aligned} \rho \dot{v}_i &= \nabla_j \sigma_{ij}, \\ \dot{\sigma}_{ij} &= q_{ijkl}\dot{\varepsilon}_{kl} + F_{ij}. \end{aligned} \tag{1}$$

Here ρ is the medium density, v_i are the components of the drift velocity vector, σ_{ij} and ε_{ij} are components of the Cochi stress and deformation tensors, ∇_j is the covariant derivative by the jth coordinate, and F_{ij} is the additional right-hand part. The appearance of the 4th-order tensor components q_{ijkl} is determined by the medium's rheology. For the linear-elastic case, they have the form

$$q_{ijkl} = \lambda\delta_{ij}\delta_{kl} + \mu(\delta_{ik}\delta_{jl} + \delta_{il}\delta_{jk}).$$

In this correlation, which generalizes Hooke's law, λ and μ are Lame's parameters, and δ_{ij} is the Kronecker delta.

The first line in the system of equations (1) represents the three equations of motion and the second line represents six rheological correlations. The vector of unknown functions, consisting of nine components, has the form

$$\mathbf{u} = \{v_1, v_2, v_3, \sigma_{11}, \sigma_{12}, \sigma_{13}, \sigma_{22}, \sigma_{23}, \sigma_{33}\}^T.$$

Then the listed models of a solid permit the system of equations (1) of the dynamics of deformable solid to be written in the matrix form [6]:

$$\frac{\partial \mathbf{u}}{\partial t} = \sum_{j=1}^{3} \mathbf{A}_j \frac{\partial \mathbf{u}}{\partial x_j}, \tag{2}$$

where $\mathbf{A}_j$ are matrices of size 9×9:

$$\mathbf{A}_1 = \begin{vmatrix} 0 & 0 & 0 & -\frac{1}{\rho} & 0 & 0 & 0 & 0 & 0 \\ 0 & 0 & 0 & 0 & -\frac{1}{\rho} & 0 & 0 & 0 & 0 \\ 0 & 0 & 0 & 0 & 0 & -\frac{1}{\rho} & 0 & 0 & 0 \\ -(\lambda+2\mu) & 0 & 0 & 0 & 0 & 0 & 0 & 0 & 0 \\ 0 & -\mu & 0 & 0 & 0 & 0 & 0 & 0 & 0 \\ 0 & 0 & -\mu & 0 & 0 & 0 & 0 & 0 & 0 \\ -\lambda & 0 & 0 & 0 & 0 & 0 & 0 & 0 & 0 \\ 0 & 0 & 0 & 0 & 0 & 0 & 0 & 0 & 0 \\ -\lambda & 0 & 0 & 0 & 0 & 0 & 0 & 0 & 0 \end{vmatrix},$$

$$\mathbf{A}_2 = \begin{vmatrix} 0 & 0 & 0 & 0 & -\frac{1}{\rho} & 0 & 0 & 0 & 0 \\ 0 & 0 & 0 & 0 & 0 & -\frac{1}{\rho} & 0 & 0 & 0 \\ 0 & 0 & 0 & 0 & 0 & 0 & -\frac{1}{\rho} & 0 & 0 \\ 0 & -\lambda & 0 & 0 & 0 & 0 & 0 & 0 & 0 \\ -\mu & 0 & 0 & 0 & 0 & 0 & 0 & 0 & 0 \\ 0 & 0 & 0 & 0 & 0 & 0 & 0 & 0 & 0 \\ 0 & -(\lambda+2\mu) & 0 & 0 & 0 & 0 & 0 & 0 & 0 \\ 0 & 0 & -\mu & 0 & 0 & 0 & 0 & 0 & 0 \\ 0 & -\lambda & 0 & 0 & 0 & 0 & 0 & 0 & 0 \end{vmatrix},$$

$$\mathbf{A}_3 = \begin{vmatrix} 0 & 0 & 0 & 0 & 0 & -\frac{1}{\rho} & 0 & 0 & 0 \\ 0 & 0 & 0 & 0 & 0 & 0 & -\frac{1}{\rho} & 0 & 0 \\ 0 & 0 & 0 & 0 & 0 & 0 & 0 & -\frac{1}{\rho} & 0 \\ 0 & 0 & -\lambda & 0 & 0 & 0 & 0 & 0 & 0 \\ 0 & 0 & 0 & 0 & 0 & 0 & 0 & 0 & 0 \\ -\mu & 0 & 0 & 0 & 0 & 0 & 0 & 0 & 0 \\ 0 & 0 & -\lambda & 0 & 0 & 0 & 0 & 0 & 0 \\ 0 & -\mu & 0 & 0 & 0 & 0 & 0 & 0 & 0 \\ 0 & 0 & -(\lambda+2\mu) & 0 & 0 & 0 & 0 & 0 & 0 \end{vmatrix}.$$

This record is the canonic form of the record of a system of equations accepted in computational mathematics to construct grid-characteristic difference schemes. The system of equations (2) is hyperbolic, so each $\mathbf{A}_j$ matrix has nine real eigenvalues and the basis of eigenvectors.

2.2. The grid-characteristic method. The grid-characteristic method [1, 7] is widely applied for the numerical modeling of the problems of the dynamics of a deformable solid. At first, use is made of the method of splitting by spatial coordinates, yielding three one-dimensional systems

$$\frac{\partial \mathbf{u}}{\partial t} = \mathbf{A_j}\frac{\partial \mathbf{u}}{\partial x_j}, \quad j = 1,2,3. \tag{3}$$

Each of these systems is hyperbolic and has a full set of eigenvectors with real eigenvalues, so each system can be rewritten as

$$\frac{\partial \mathbf{u}}{\partial t} = \mathbf{\Omega_j^{-1}\Lambda_j\Omega_j}\frac{\partial \mathbf{u}}{\partial x_j},$$

where matrix $\mathbf{\Omega_j}$ is a matrix composed of eignevectors and $\mathbf{\Lambda_j}$ is the diagonal matrix whose elements are eigenvalues. For all the coordinates, matrix $\mathbf{\Lambda}$ appears as

$$\mathbf{\Lambda} = \mathrm{diag}\{c_p, -c_p, c_s, -c_s, c_s, -c_s, 0, 0, 0\},$$

where $c_p = \sqrt{(\lambda+2\mu)/\rho}$ is the longitudinal sound velocity in the medium and $c_s = \sqrt{\mu/\rho}$ is the transverse sound velocity.

After the substitution of variables $\mathbf{\nu} = \mathbf{\Omega u}$, each of systems (3) splits into nine independent scalar transport equations (index j is omitted below, where possible)

$$\frac{\partial \mathbf{\nu}}{\partial t} + \mathbf{\Lambda}\frac{\partial \mathbf{\nu}}{\partial x} = 0.$$

One-dimensional transport equations are solved by means of the method of characteristics or by ordinary finite-difference schemes.

Once all the $\mathbf{\nu}$ components are transported, the solution itself is restored

$$\mathbf{u^{n+1}} = \mathbf{\Omega^{-1}\nu^{n+1}}.$$

Here, we used the TVD-difference schemes [8] of the 2nd order of accuracy. In the program, 15 different limiters [9] have been implemented, in the calculations the limiter superbee, proposed in [10], was mostly used:

$$\phi_{sb}(r) = \max[0, \min(2r,1), \min(r,2)].$$

Use was also made of grid-characteristic monotonic difference schemes, whose principle of construction is described in [2]. The program implements the schemes of the 2nd–4th order of accuracy; most calculations were carried out using the scheme of the 4th order of accuracy. We give it for the case of the numerical solution of the one-dimensional linear elasticity equation $u_t + \lambda u_x = 0$, $\sigma = \lambda\tau/h$:

$$u_m^{n+1} = u_m^n - \sigma(\Delta_1 - \sigma(\Delta_2 - \sigma(\Delta_3 - \sigma\Delta_4))),$$

$$\Delta_1 = \frac{1}{24}(-2u_{m+2}^n + 16u_{m+1}^n - 16u_{m-1}^n + 2u_{m-2}^n),$$

$$\Delta_2 = \frac{1}{24}(-u_{m+2}^n + 16u_{m+1}^n - 30u_m^n + 16u_{m-1}^n - u_{m-2}^n),$$

$$\Delta_3 = \frac{1}{24}(2u_{m+2}^n - 4u_{m+1}^n + 4u_m^n - 2u_{m-2}^n),$$

$$\Delta_4 = \frac{1}{24}(u_{m+2}^n - 4u_{m+1}^n + 6u_m^n - 4u_{m-1}^n + u_{m-2}^n).$$

In addition, use is made of the grid-characteristic criterion of monotony [2]. In the case of the positive value λ, the monotony criterion is

$$\min\left\{u_m^n, u_{m-1}^n\right\} \le u_m^{n+1} \le \max\left\{u_m^n, u_{m-1}^n\right\}.$$

For negative values, λ, it will be symmetrical. In the simplest implementation, use is made of the limiter

$$u_m^{n+1} = \begin{cases} \max\left\{u_m^n, u_{m-1}^n\right\}, & u_m^{n+1} > \max\left\{u_m^n, u_{m-1}^n\right\}, \\ \min\left\{u_m^n, u_{m-1}^n\right\}, & u_m^{n+1} < \min\left\{u_m^n, u_{m-1}^n\right\}. \end{cases}$$

In [2] it is shown that this limiter maintains the 4th order in domains where the solution behaves sufficiently smoothly (the characteristic criterion holds), in case of larger gradients of the solution, the order of the scheme is reduced to the 3rd.

3. PROGRAM COMPLEX

For modeling the problems of the propagation of wave disturbances in layered geological media, a program complex has been created to solve the stated problems numerically by using the grid-characteristic methods of various orders of approximation.

In the creation of the software package, one of the basic requirements was the possibility for computations at sufficiently large computation grids (about 1 billion nodes) in order to have an opportunity to model in large domains of terrestrial rock. In this case, there are considerable requirements for both resources of the processor time and short-term memory of the computer. For parallelization of the algorithm work, the technology of writing the program in the apportioned MPI cluster medium [5] is used.

Figure 1 shows a graph of the acceleration of the program with an increased number of processor cores on which the calculation is made.

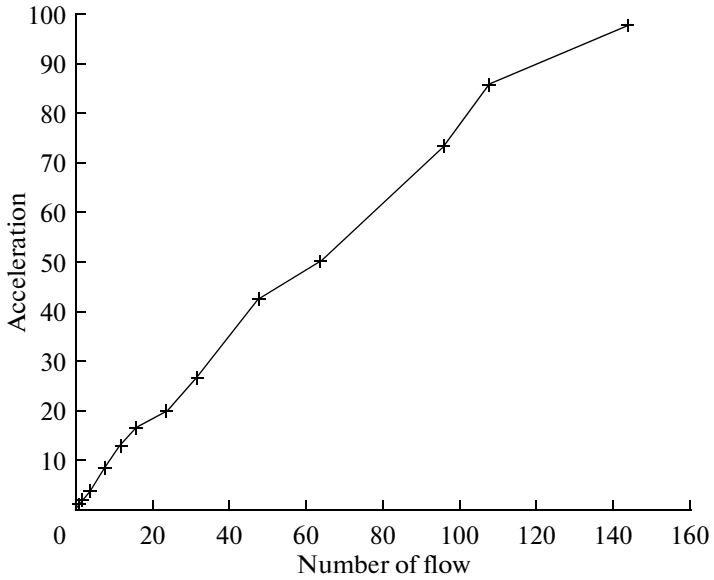

Fig. 1. Schedule of acceleration using MPI technology on a grid of 64 million nodes.

In the acceleration test, a calculation grid with 64 million nodes was used. The test shows good acceleration (97.5 times on 144 cores) and the efficiency of operation of the parallel algorithm (up to 70% on 144 cores).

Since all the solvable problems are dynamic, in operating the program, large data arrays that represent the distribution of physical parameters in different time moments need to be saved. To accelerate and simplify the work with files in distributed systems, the technology of parallel operation with the MPI IO file system was applied, thus improving the efficiency and convenience for the end user while maintaining large volumes of data.

4. RAYLEIGH WAVES

The Rayleigh waves appear on the boundary of a half-plane filled with a homogenous isotropic elastic medium. Theoretically, these waves were found by Rayleigh in 1885, and they can exist near a free boundary of a solid body bordering a vacuum or a sufficiently rarefied gas medium. The phase velocity of such waves is directed in parallel to the boundary, and the near oscillating particles of the medium have both transverse and longitudinal normals to the surface components of the displacement vector. The phase velocity of the Rayleigh waves does not depend on the wave length; i.e., they are not dispersive. These waves decay very fast by the depth of the semiplane [12], due to the presence of exponential factors with the exponent $-q\alpha z$, where q is the wave number, z is the coordinate directed to the depth of the semiplane, and α is the multiplier dependent on the parameters of the medium and the Rayleigh wave velocity. From this it follows that the lower the wave length (a higher wave number) the faster is decay. It turns out that the Rayleigh waves are superficial; i.e., their basic energy is concentrated at the boundary.

The Rayleigh waves are of great interest for seismologists since they are seen at a distance from the center of earthquakes, and, like the Love waves, are the cause for destruction of surface facilities.

We use c_p and c_t to denote the longitudinal and transverse velocity, respectively, in the medium, and c_R to denote the Rayleigh waves. The correlation between these velocities is set by an equation in the third degree [11]:

$$f(\xi) = \xi^3 - 8\xi^2 + 8(2+\chi)\xi - 8(1+\chi) = 0, \tag{4}$$

where

$$\xi = c_R^2/c_t^2, \quad \chi = 1 - \frac{2^2}{\eta}, \quad \eta = \frac{c_p}{c_t}.$$

As is known, for all the elastic bodies the inequality $0 < \eta < \sqrt{2}$ holds; taking this into account, the analysis of (4) shows that $0.8741 < \sqrt{\xi} < 0.9554$. Thus, the velocity of the Rayleigh waves differs little from the velocity of the shear waves, but always less than it.

We can write down the explicit form of the roots of Eq. (4) for some special values of the elastic constants of the medium [11]

1. $\chi = 0, \ \eta^2 = 2, \ \xi = 3 - \sqrt{5}$.

2. $\chi = 1/3, \ \eta^2 = 3, \ \xi = 2(1 - 1/\sqrt{3})$—Cauchy medium.

The main purpose of this simulation was to obtain Rayleigh waves and to compare them by the numerical method of velocities with the velocities from Eq. (4). This test involved the two special cases described above.

The computational domain for all tests was a parallelepiped with dimensions $1500 \times 500 \times 200$ m along the x, y and z axes, respectively. On the top edge by axis z there was a boundary condition of absorption. The grid step in all calculations was taken of an order of 10 m and the number of nodes in the grid was about 160000. The integration step in time was chosen proceeding from the fulfillment of the Courant condition; in all tests it is 0.001615 s.

The first calculation was performed with the following parameters of the medium: $c_t = 2000$ m/s and $c_p = \sqrt{2}c_t \approx 2830$ m/s. The rated speed of the Rayleigh waves in this case will be $c_R = \sqrt{3-\sqrt{5}}c_t \approx 0.874c_t \approx 1748$ m/s. Figure 2 shows a crosssection passing through the middle of the calculation domain parallel to the x and z axes and normal to the y axis. The velocity modules are given for the time moments $t = 0.2955$ and $t = 0.6412$ s.

In the pictures the propagation of the surface wave is clearly seen: with the depth of penetration, the wave is strongly damped and the maximum amplitude is at the medium surface. During this time the wave

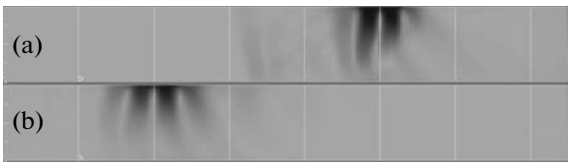

Fig. 2. Propagation of the Rayleigh wave in the first case: (a) $t = 0.2955$ s, (b) $t = 0.6412$ s.

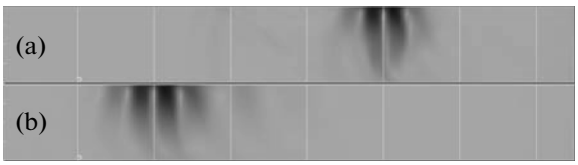

Fig. 3. Propagation of the Rayleigh wave in the second case: (a) $t = 0.2794$ s, (b) $t = 0.6089$ s.

has propagated at 600 m, it is easy to calculate its phase velocity: $c = 1736$ m/s. This figure is closely correlated to the theoretical value (1748 m/s) obtained earlier.

In the second calculation, the cross-section velocity was also the same and the longitudinal $c_p = \sqrt{c_t} \approx$ 3464 m/s; the theoretical velocity of the Raileigh wave in this case will be $c_R = \sqrt{2(1-1/\sqrt{3})}c_t \approx 0.9194c_t \approx$ 1839 m/s. Figure 3 presents similar cross sections for the time moments $t = 0.2794$ and $t = 0.6089$ s.

The wave picture is similar to the picture obtained in the former case, it is also easy to obtain the value of the velocity of the wave $c = 1821$ m/s, which well agrees with the theoretical value. Base on the obtained results, it is possible to conclude that the calculation data agree with the theory.

5. LOVE WAVES

In layered media the appearance of a certain type of waves, i.e., Love waves, is possible. The shear vector in such waves is parallel to the boundary of the division of the media and is normal to the direction of the propagation; i.e., Love waves have horizontal polarization. Unlike the Rayleigh waves arising in the same half-space with the free boundary, the Love waves arise in elastic layer type structures on an elastic half-space. The theory of these eponymous waves was given by Love in 1911. In seismic practice, these waves are well known, as they are the major cause for destruction of the base plates of facilities and for the appearance of large cracks and rifts on the earth's surface.

To get the expression for the wave speed in an explicit form [11] is a problem; we therefore define the wave by indirect signs and check the correlation of the speed and wave length to fulfill the Love wave equation. The speed of the Lave wave propagation will be denoted by c_L. Then, the relationship

$$c_{t1} < c_L < c_{t2}, \tag{5}$$

where c_{t1} and c_{t2} are cross-sectional sound velocities for the upper layer and half-space, respectively, is fulfilled for it. From this it follows that for existence of the Love waves, it is necessary that the cross-sectional sound velocity in the matter of the layer is less than the cross-sectional sound velocity in the half-space matter. Also, unlike the Rayleigh waves, the Love waves have dispersion; i.e., they depend on frequency and do not keep the form of the impulse. The wave amplitude in the half-space attenuates exponentially.

We denote through H the thickness of the upper layer, ω is the angular frequency of the Love wave, $\chi_1^2 = \omega^2/c_{t1}^2$, $\chi_2^2 = \omega^2/c_{t2}^2$. Then, the finite number of the Love waves (number of possible harmonics) in the superficial layer is determined by the relation

$$N = \left[H\sqrt{\chi_1^2 - \chi_2^2}/\pi \right] + 1. \tag{6}$$

Here, $[a]$ denotes the integer part of number a. Substituting into (6) the expression for χ_1 and χ_2, and taking into account $\omega = 2\pi c_L/\lambda_L$, where λ_L is the length of the Love wave, we obtain

$$N = \left[\frac{2Hc_L}{\lambda_L}\sqrt{\frac{1}{c_{t1}^2} - \frac{1}{c_{t2}^2}} \right] + 1. \tag{7}$$

We write the equation determining the properties of the surface Love waves:

$$\tan\eta = (\mu_2/\mu_1)\left[(\chi_1 H)^2 - (\chi_2 H)^2 - \eta^2 \right]^{1/2} \eta. \tag{8}$$

Here, μ_2 and μ_1 are elastic Lame constants for the half-space and the layer, respectively, $\eta = \sqrt{\chi_1^2 - \xi^2}H$ and $\xi^2 = \omega^2/c_L^2$. This equation determines the correlation between velocity and the Love wave's length.

The main target of simulation was to get the Love waves in the near-surface layer and determine by the indirect attributes described above whether the obtained wave is actually a Love wave.

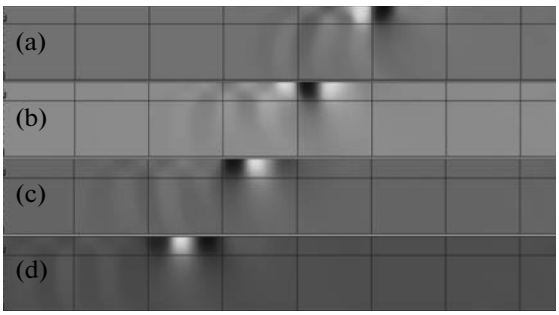

Fig. 4. Propagation of the Love wave: (a) $t = 0.258$ s, (b) $t = 0.347$ s, (c) $t = 0.436$ s, (d) $t = 0.525$ s.

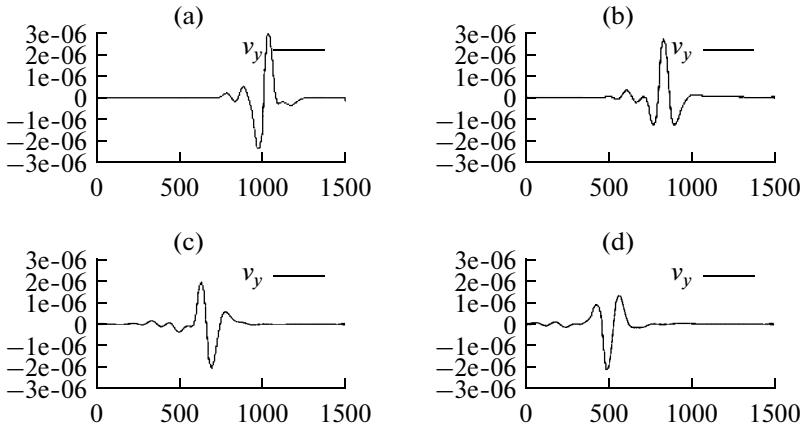

Fig. 5. Component y of the medium speed at the layer surface: (a) $t = 0.258$ s, (b) $t = 0.347$ s, (c) $t = 0.436$ s, (d) $t = 0.525$ s.

The calculated area has the aspect of two parallelepipeds, presenting the upper layer and low half-space; their sizes are $1500 \times 500 \times 50$ m ($H = 50$ m) and $1500 \times 500 \times 150$ m by axes x, y, and z, respectively. On the upper face of the layer, the boundary condition was exposed by axis z, and on the other faces of the layer and half-space, the boundary condition of absorption was established. Between the layer and half-space, the condition of the contact boundary is established. The grid step was equal to 10 m, the number of nodes in the grid was about 170000. The integration step in time was chosen proceeding from the fulfillment of the Courant condition; in this text, it is 0.001615 s.

In the calculation, the following parameters of the medium were used (index 1 refers to the upper layer, index 2 refers to the half-space): $c_{p1} = 3000$ m/s, $c_{t1} = 2000$ m/s, $c_{p2} = 6000$ m/s, $c_{t2} = 3000$ m/s, and $\rho_1 = \rho_2 = 2500$ kg/m^3. Figure 4 shows the section passing through the middle of the computational domain, parallel to axes x and z and normal to axis y. The shaded part shows the y components of the velocity for the time moments 0.258, 0.347, 0.436, and 0.525 s.

As seen from the graphs, the obtained wave has horizontal polarization and attenuates very soon in the half-space. The propagation occurs along the surface layer and the form of impulse changes. It is easy to calculate the velocity of the obtained wave: $c = 600/(0.525 - 0.258) = 2247$ m/s, as is seen, satisfies correlation (5).

For a more detailed study, we present one-dimensional graphs of the y component of velocity near the layer surface along the x axis for analogous time moments; they are shown in Fig. 5.

In the graphs the value of the x and z components are not shown since actually they are zero. The disturbance is only seen in the y component of the velocity. Over all the time of computation seen one period of the wave is well, although the form of impulse changes. The length of the obtained wave is of an $\lambda_L = 140$ m order, which is seen from the graph.

Substituting into formula (7) the obtained values, i.e., velocity of propagation, length of wave and parameters of the computation medium, we obtain the Love wave number: $N = [0.5992] + 1 = 1$; this shows that there should exist only one harmonic and equation (8) has only one real root.

Parameters of a layered medium

H, m	V_p, km/s	V_s, km/s
300	4.19	2.79
400	4.65	3.1
500	5.85	3.5
2800	6.13	3.9

Equation (8) is transcendental; thus, it is not possible to obtain explicitly the value for the angular frequency of the Love wave. We find an approximated value of the angular frequency of the Love wave from the equation numerically. Thus, $\omega_{\text{theor}} \approx 107.7$ Hz. Earlier, the value of the Love wave length, $\lambda_L = 140$ m, had been already obtained; from this we have the experimental values of the frequency: $\omega_{\text{exp}} = 2\pi c_L/\lambda_L = 101$ Hz. It is seen that the theoretical value differs from the experimental one by not more than 10%.

6. SIMULATION OF PROPAGATION OF DISTURBANCES FROM THE HYPOCENTER OF EARTHQUAKE

In this work, the process of the propagation of elastic waves arising in an earthquake in heterogenous media is investigated.

For simulation the focus of the earthquake, a shear model of perturbation in the hypocenter was chosen. In this model an angular domain 40 m wide and 500 m long with some nonzero velocity was set. One part of the area is moving in one direction, the other in the opposite direction. Such a model physically corresponds to the situation where there is a rift in the earth's crust in which the travel in the earthquake takes place. In this work, we compared the propagation of disturbances from two types of earthquakes, i.e., with horizontal and vertical shear.

The choice of the module value of velocity was made by comparison of the simulation data and real experimental data. The data were taken from the earthquake that had taken place near Guadalupe Victoria on July 6, 2010. According to estimates by the automatic system, the center of the earthquake was at a depth of 1.5 km. From the map of maximum velocities, it is known that maximal velocities of the soil on the earth's surface were of an order of 1 cm/s. By assigning different values of velocity in the focus of the earthquake and using numerical simulation, it was found that to obtain the amplitudes of velocities on the surface of the same order, it is necessary to assign the speed of the initial perturbation equal to 10 cm/s.

Simulation of the propagation of waves in an earthquake occurring in a layered medium was performed. The density of all the layers was taken as constant and equal to 2500 kg/m^3. The thicknesses of the layers and the velocities of longitudinal and transversal waves are given in Table 1.

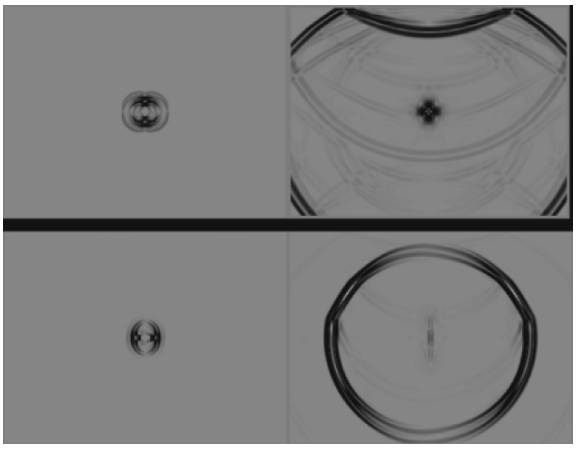

Fig. 6. Results of modeling for an earthquake with horizontal and vertical shear (from top to bottom).

Figure 6 shows the distributions of the velocity module in the propagation of waves from the hypocenter to the day surface for earthquakes with horizontal and vertical shears.

The results are presented for the same moments of time. The strong second front of the transversal wave is clearly seen; it has a lower velocity and it reaches the earth's surface later. Also noticeable are the retractions from various geological layers. The pictures from different perturbation views differ and have good qualitative agreement with the experimental data.

7. CONCLUSIONS

The computations carried out show the possibility of using the developed numerical methods for simulation of various seismic phenomena and the passage of elastic waves in complicated constructions. The used grid-characteristic method on parallelepiped grids

makes it possible to correctly stage conditions on the boundaries of the integration domain and on the boundaries of the contacts of grids and, due to the developed grid-characteristic scheme of a higher order of accuracy, to simulate dynamic wave processes in large computation domains. The combination of rectangular grids makes it possible to set the layered media and this allows application of this method to simulate the Rayleigh and Love waves; the obtained results have yielded good agreement with the theory. The simulation of a disturbance from the hypocenter of the earthquake to the earth's surface was made in a layered heterogeneous geological medium. The created software complex is parallelized to work in the medium of the distributed cluster and optimized for work with large arrays of data.

ACKNOWLEDGMENTS

The work was performed with the financial support of the Russian Ministry of Education and Science within state contract no. 14.515.11.0069.

REFERENCES

1. K. M. Magomedov and A. S Kholodov, *Grid-Characteristic Numerical Methods* (Nauka, Moscow, 1988).
2. A. S. Kholodov and Ya. A. Kholodov, " On criteria of monotony of difference schemes for equation of hyperbolic type," Comput. Math. Math. Phys. **46** (9) 1560–1588 (2006).
3. I. B. Petrov, A. G. Tormasov, and A. S. Kholodov, "Numerical study of unsteady processes in deformable media of the multilayer structure," Izv. Akad. Nauk SSSR, Solid Dyn., No. 4, 89–95 (1989).
4. Ye. Kvasov, S. A. Pankratov, and I. B. Petrov, "Numerical simulation of seismic response in multilayered geological media by the grid-characteristic method," Math. Models Comput. Simul. **22** (9) 13–21 (2010).
5. MPI Forum. Message Passing Interface (MPI) Forum Home Page. http://www.mpi-forum.org/ (2009).
6. I. B. Petrov and A. S. Kholodov, "Numercial study of some dynamic problems of solid mechanics by the grid-characteristic method," Comput. Math. Math. Phys. **24** (5) 722–739 (1984).
7. K. M. Magomedov and A. S. Kholodov, "On construction of difference schemes for equations of the hyperbolic type on the basis of characteristic correlations," Comput. Math. Math. Phys. **9** (2) 373–386 (1969).
8. Ami Harten, "High resolution schemes for hyperbolic conservation laws," J. of Comp. Physics **135** (2) 260–278 (1997).
9. I. B. Petrov and N. I. Khokhlov, "Comparison of TVD limiters for numerical solution of equations of the dynamics of the deformable solid by grid-characteristic method," *Mathematical Models and Problems of Control* (MFTI, Moscow, 2011), pp. 104–111 [in Russian].
10. P. L. Roe, "Characteristic-based schemes for the Euler equations," Annual Review of Fluid Mechanics, No. 18, 337–365 (1986).
11. A. G. Gorshkov, A. L. Medvedskii, L. N. Rabinskii, and D. V. Tarlakovskii, *Waves in continuous media* (Fizmatlit, Moscow, 2004) [in Russian].
12. L. M. Brekhovskikh and V. V. Goncharov, *Introduction in Mechanics of Continuous Media* (Nauka, Moscow, 1982) [in Russian].

Translated by D. Shtirmer

SPELL: 1. OK